Dynamic Analysis of a Moderately Thick Plate on Pasternak Type Foundation under Impact and Moving Loads

Neslihan Genckal, Reha Gursoy, Vedat Z. Dogan

Abstract—In this study, dynamic responses of composite plates on elastic foundations subjected to impact and moving loads are investigated. The first order shear deformation (FSDT) theory is used for moderately thick plates. Pasternak-type (two-parameter) elastic foundation is assumed. Elastic foundation effects are integrated into the governing equations. It is assumed that plate is first hit by a mass as an impact type loading then the mass continues to move on the composite plate as a distributed moving loading, which resembles the aircraft landing on airport pavements. Impact and moving loadings are modeled by a mass-spring-damper system with a wheel. The wheel is assumed to be continuously in contact with the plate after impact. The governing partial differential equations of motion for displacements are converted into the ordinary differential equations in the time domain by using Galerkin's method. Then, these sets of equations are solved by using the Runge-Kutta method. Several parameters such as vertical and horizontal velocities of the aircraft, volume fractions of the steel rebar in the reinforced concrete layer, and the different touchdown locations of the aircraft tire on the runway are considered in the numerical simulation. The results are compared with those of the ABAQUS, which is a commercial finite element code.

Keywords—Elastic foundation, impact, moving load, thick plate.

I. INTRODUCTION

NUMEROUS flights are operated each day for both military and civil purposes. Airport runways should be designed so as to provide safe landing, takeoff, and taxi operations. Runway characteristics may be different and are generally affected by the composition of the runway itself and the soil under the runway. Also, the deformations and the stresses within the runway depends on the runway and soil characteristics, air traffic frequency, the type of the landing aircraft, etc.

In this study, the dynamic responses of a runway are investigated. The solutions are obtained by using both the 'analytical' and the numerical solutions. In the numerical solution, the aircraft is modeled as a point mass, in which the total aircraft mass is divided among the tires in contact with the runway to obtain the apportioned mass acting on each tire. The deformations and the contact pressures at the instants of the touchdown and the continuing motion are obtained from the ABAQUS simulations. These contact pressures are then substituted back into the governing equations of motion in the analytical solution. A selected number of analytical and numerical cases are compared in order to see if there is an agreement between the two solutions. The deformations and the stresses within the plate are obtained for different vertical and horizontal velocities of the aircraft, volume fractions of the steel rebar in the reinforced concrete layer, and for touchdown locations of the aircraft tire to the runway.

II. LITERATURE REVIEW

Bogacz and Cyzczula [1] studied the dynamical response of a Timoshenko beam with a Winkler type viscoelastic foundation beneath. Özgan and Daloğlu [2] conducted a research to analyze the dynamic response of thick plates on a two parameter elastic foundation under time variable loading. They used Kirchoff plate theory to model the plate and Vlasov model as the foundation model and solved the problem via the finite element method. Idowu et al. [3] investigated the dynamic effects of the viscous damping for an isotropic rectangular plate which is on a Pasternak type elastic foundation and also subjected to moving load. Gibigaye et al. [4] examined the dynamic response of a rigid thin plate on a Pasternak-Vlasov foundation model to find the loading conditions of a highway. They used the Bolotin method to find the natural frequencies and the mode shapes. Maamar et al. [5] used LS-DYNA to analyze a laminated composite plate subjected to a low speed impact load for different tilt angles. Lee et al. [6] investigated a circular composite plate subjected to low velocity impact load. They presumed a quasi-isotropic plate and used the nonlinear Rayleigh-Ritz method for the analytical modeling.

III. THEORETICAL FORMULATION

A. Runway Structure

As it is shown in Fig. 1, the runway is modeled as a composite plate with four layers. The layers of the runway are: A surfacing course, a (reinforced concrete) base layer, a foundation soil (subbase) and a soil support, respectively from top to the bottom.

Neslihan Genckal was a research assistant in the department of Aeronautical Engineering at Istanbul Technical University, Maslak 34469, Istanbul, Turkey. She is currently a graduate student in the department of Civil Engineering and Engineering Mechanics at Columbia University, New York, NY 10027, US (phone: +1-929-215-1648; e-mail: ng2618@columbia.edu).

Reha Gursoy is an MS graduate from the department of Aeronautics and Astronautics Engineering, Istanbul Technical University, Maslak 34469, Istanbul, Turkey (e-mail: engr.rehagursoy@gmail.com).

Vedat Z. Dogan is a professor in the department of Aeronautical Engineering, Istanbul Technical University, Maslak 34469, Istanbul, Turkey (e-mail: doganve@itu.edu.tr).

TABLE I
MATERIAL PROPERTIES OF THE RUNWAY LAYERS

Layer	Thickness (m)	Young's Modulus (GPa)	Shear Modulus of Elasticity (GPa)	Density (kg/m³)	Poisson's Ratio
Surfacing course	0.1	5.4	3.07	2446	0.35
Base layer	0.1	87.52	$G_{12}=G_{13}=13.64$ $G_{23}=12.86$	2978	0.22
Subbase layer	0.3	0.26	0.15	2518	0.38
Soil support	0.3	0.12	0.08	1835	0.48
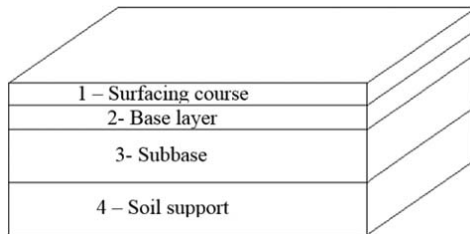
Fig. 1 The layers of the runway

The material properties of the runway layers are given in Table I [7]. The second layer (base layer) of the runway is composed of steel rebar as fiber and concrete as matrix material. The material properties of the reinforced concrete layer are obtained by using the rule of mixtures. The volume fraction of the steel rebar in the reinforced concrete layer is taken as 0.2 for the base case.

B. Soil Properties

The soil under the runway is modeled by using the Pasternak-type foundation. In this study, the equivalent spring (k_w) and damping coefficients (k_g) for the soil are taken as 1.3634×10^{10} N/m and 3.4085×10^{10} N.s/m, respectively. These coefficients are calculated from (1) and (2) where the non-dimensional spring and damping coefficients of $K_w=100$ and $K_g=10$ are taken as in [8].

$$k_w = K_w \frac{D_{11}}{a^4} a \cdot b \qquad (1)$$

$$k_g = K_g \frac{D_{11}}{a^2} a \cdot b \qquad (2)$$

where D_{11} is the bending stiffness of the composite material, a and b are the length and width of the runway, respectively.

C. Aircraft and Landing Gear

Boeing B747-400 is used to model the impact and the moving load on the runway. The maximum landing mass of aircraft is given as 295,743 kg. [9]. Main gear of B747-400 has 16 tires. The load of the aircraft is divided equally between the 16 main gear tires for the analyses. In this case, a mass of 18,484 kg is considered to be acting on each tire.

The total spring and damping coefficient for the B747-400 main landing gear are 5×10^6 N/m and 5.473×10^6 N.s/m, respectively [10]. Springs and dampers are assumed to be parallel. This makes one spring and dashpot coefficient on each tire $k=1.25 \times 10^6$ N/m and $C=1.368 \times 10^6$ N.s/m, respectively.

The aircraft body-landing gear-tire assembly model is shown in Fig. 2.
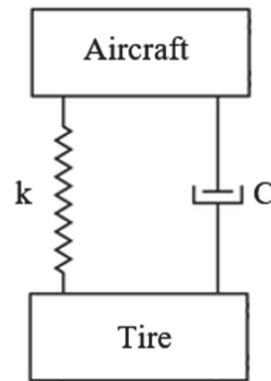

Fig. 2 The assembly of aircraft and the tire

D. Tire Properties

The main gear tire size of the B747-400 is H49x19.0-22. The main gear tire pressure is given between 190-200 psi (1.3-1.4 MPa) [11]. In this study, it is taken as 1.3 MPa. For simplicity, the tire is modeled as an assembly of rubber and steel materials, no fabrics are used. The constituents of the tire model, which are a rubber part, a reinforcing ply, a steel bead and a rim are shown in Figs. 3 (a)-(d), respectively.
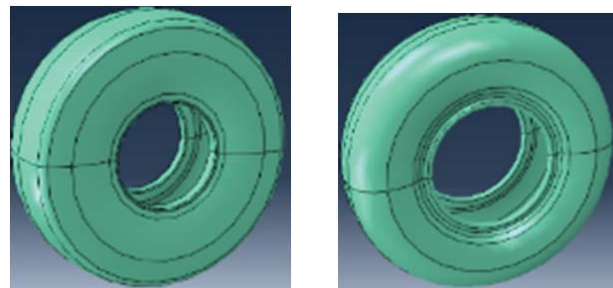
(a) The rubber part   (b) The reinforcing ply
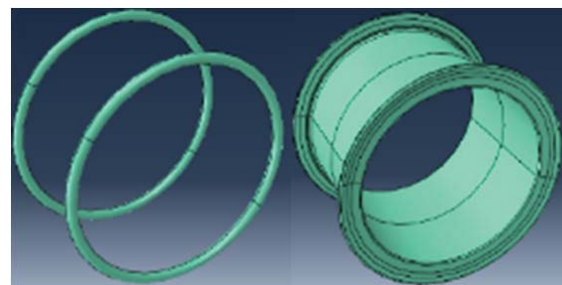
(c) The steel bead   (d) The rim

Fig. 3 Constituents of the tire

E. Equation of Motion of the Plate

In this study, it is assumed that in-plane displacements and inertias are smaller than out-of-plane displacements/rotations and inertias. Therefore, the in-plane motion is neglected and the equations of motion are reduced from a set of five equations to a set of three equations. The equations of motion of a rectangular composite plate in terms of displacements by using the FSDT, with added structural damping for the plate itself and the spring and dashpots of the foundation model and with some eliminated terms, can be written as in (3)-(5) [12],

$$K \cdot A_{44}\left(\frac{\partial^2 w_0}{\partial y^2} + \frac{\partial \phi_x}{\partial y}\right) + K \cdot A_{55}\left(\frac{\partial^2 w_0}{\partial x^2} + \frac{\partial \phi_y}{\partial x}\right) \tag{3}$$
$$+ k_w w_0 + k_g\left(\frac{\partial^2 w_0}{\partial x^2} + \frac{\partial^2 w_0}{\partial y^2}\right) + p(x,y,t) = I_0 \frac{\partial^2 w_0}{\partial t^2} + \lambda \frac{\partial w_0}{\partial t}$$

$$D_{11}\frac{\partial^2 \phi_x}{\partial x^2} + D_{66}\left(\frac{\partial^2 \phi_x}{\partial y^2} + \frac{\partial^2 \phi_y}{\partial y \partial x}\right) - K \cdot A_{55}\left(\frac{\partial w_0}{\partial x} + \phi_x\right) \tag{4}$$
$$= I_2 \frac{\partial^2 \phi_x}{\partial t^2} + \lambda \frac{\partial \phi_x}{\partial t}$$

$$D_{22}\frac{\partial^2 \phi_y}{\partial y^2} + D_{66}\left(\frac{\partial^2 \phi_y}{\partial x^2} + \frac{\partial^2 \phi_x}{\partial x \partial y}\right) - K \cdot A_{44}\left(\frac{\partial w_0}{\partial y} + \phi_y\right) \tag{5}$$
$$= I_2 \frac{\partial^2 \phi_y}{\partial t^2} + \lambda \frac{\partial \phi_y}{\partial t}$$

where K is the shear correction factor, A_{ij} are the extensional and D_{ij} are the bending stiffnesses of the composite plate, w_0 is the mid-plane displacement in the z (vertical) direction, φ_x and φ_y are the rotations about y and x-axis, k_w is the coefficient of foundation stiffness along z direction, k_g is the coefficient of shearing layer of elastic foundation, p(x,y,t) is the pressure load acting on the top surface of the plate, λ is the damping coefficient of the plate, I_0 and I_2 are the mass moments of inertia of the plate. A_{ij} and D_{ij} can be expressed as given in (6) [12]:

$$A_{ij}, D_{ij} = \int_{-\frac{h}{2}}^{\frac{h}{2}} \bar{Q}_{ij}^k (1, z^2)\, dz \tag{6}$$

$$i,j = 1,2,6 \ for\ D_{ij}$$

$$i,j = 4,5 \ for\ A_{ij}$$

where, $\bar{Q}_{ij}^k$ are the reduced stiffness coefficients of the kth layer of the composite structure.

The mass moment of inertias I_0 and I_2 are defined as in (7);

$$I_0, I_2 = \int_{-\frac{h}{2}}^{\frac{h}{2}} (1, z^2)\, \rho^k dz \tag{7}$$

where ρ^k is the density of the kth layer of the composite.

The pressure load p(x,y,t) may be divided into two different sequence parts in time: first one is at the instant of landing (impact load) and the second one is for the moving load which immediately follows the first one.

The pressure load, which includes both definitions for the instant of landing (impact loading (p_1(x, y))) and the moving load portion (p_2(x, y)) of the loading is given in (8);

$$p(x,y,t) = \begin{bmatrix} p_1(x,y)\{u(t - t_1) - u(t - t_2)\} \\ + p_2(x,y)\{u(t - t_2)\} \end{bmatrix} \tag{8}$$

where, t_1 is the time that impact load starts and t_2 is the time that the impact load ends, and the load variation during impact is approximated as constant. That is, t_2-t_1 is the impact duration as shown in Fig. 4. After landing, the moving load starts acting as a uniform load. Spatial dependency of pressures $P_1(x,y)$ and $P_2(x,y)$ is the function of the position of the footprint of the aircraft tire on the runway.

The step function u(t-t_n) is here defined in (9):

$$u(t - t_n) = \begin{cases} 0, t < t_n \\ 1, t > t_n \end{cases} \tag{9}$$
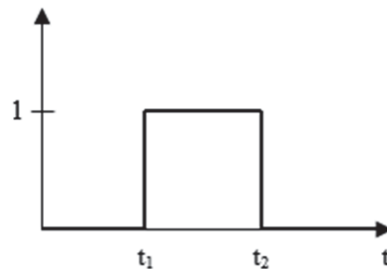

Fig. 4 The sketch for the load step function

IV. SOLUTION METHODS

A. Analytical Solution

The Navier's solution (Series expansion method) is employed for the analytical solution method. The expansions in (10)-(12) for the deflection, rotations and the time-dependent pressure load are used so as to satisfy the boundary conditions. w, φ_x and φ_y represent the transverse deflection and rotations around x and y-axis, respectively.

$$w(x,y,t) = \sum_{m=1}^{\infty}\sum_{n=1}^{\infty} W_{mn}(t) \sin\left(\frac{m\pi x}{a}\right)\sin\left(\frac{n\pi y}{b}\right) \tag{10}$$

$$\phi_x(x,y,t) = \sum_{m=1}^{\infty}\sum_{n=1}^{\infty} X_{mn}(t) \cos\left(\frac{m\pi x}{a}\right)\sin\left(\frac{n\pi y}{b}\right) \tag{11}$$

$$\phi_y(x,y,t) = \sum_{m=1}^{\infty}\sum_{n=1}^{\infty} Y_{mn}(t) \sin\left(\frac{m\pi x}{a}\right)\cos\left(\frac{n\pi y}{b}\right) \tag{12}$$

where $W_{mn}(t)$, $X_{mn}(t)$ and $Y_{mn}(t)$ are (m,n) modal amplitude coefficients of the transverse deflection and rotations about y and x-axis, respectively, which are functions of time.

After implementing the expansions given in (10)-(12) into the equations of motion given in (3)-(5) and applying Galerkin's method to obtain the differential equations of plate in time domain, one obtains the equations of motion in time domain as in (13)-(15):

$$\ddot{W}_{mn}(t) + 2\xi\omega_{mn}\dot{W}_{mn}(t) + \frac{1}{I_0}\left\{\begin{bmatrix} K \cdot A_{55} \cdot \alpha^2 + \\ (K \cdot A_{44} + k_w)\beta^2 \\ +k_g(\alpha^2 + \beta^2) \end{bmatrix}W_{mn}(t) \\ +K \cdot A_{55} \cdot \alpha \cdot X_{mn}(t) \\ +K \cdot A_{44} \cdot \beta \cdot Y_{mn}(t)\right\} =$$

$$\frac{1}{I_0\pi^2}\frac{16}{a \cdot b}\sin\left(\frac{m\pi K_2}{a}\right)\sin\left(\frac{r\pi K_1}{b}\right) \qquad (13)$$

$$\left\{\begin{matrix} P_1\left(\sin\left(\frac{m\pi x_1^*}{a}\right)\sin\left(\frac{r\pi y_1^*}{b}\right)\right) + \\ P_2\left(\sin\left(\frac{m\pi x_2^*}{a}\right)\sin\left(\frac{r\pi y_2^*}{b}\right)\right) \end{matrix}\right\} \ddot{X}_{mn}(t) + 2\xi\omega_{mn}\dot{X}_{mn}(t) +$$

$$[D_{11} \cdot \alpha^2 + D_{66} \cdot \beta^2 + K \cdot A_{55}]X_{mn}(t) \qquad (14)$$

$$[D_{12} + D_{66}]\alpha \cdot \beta \cdot Y_{mn}(t) + K \cdot A_{55} \cdot \alpha \cdot W_{mn}(t) = 0$$

$$\ddot{Y}_{mn}(t) + 2\xi\omega_{mn}\dot{Y}_{mn}(t) + [D_{22} \cdot \beta^2 + D_{66} \cdot \alpha^2 + K \cdot A_{44}]Y_{mn}(t) \qquad (15)$$

$$[D_{12} + D_{66}]\alpha \cdot \beta \cdot X_{mn}(t) + K \cdot A_{44} \cdot \beta \cdot W_{mn}(t) = 0$$

where ξ is the damping ratio, ω_{mn} are the natural frequencies of the (m,n) modes of the plate (runway), P_1 and P_2 are the average uniform pressure on the runway under the footprint of the aircraft tire during impact loading and moving loading respectively, K_1 and K_2 are the dimensions of the footprint of the aircraft tire on the runway in x and y-directions, respectively. The definitions of α and β are given in (16), (17);

$$\alpha = \frac{m\pi}{a} \qquad (16)$$

$$\beta = \frac{n\pi}{b} \qquad (17)$$

The x_1^* and y_1^* are the positions of the aircraft on the runway at the instant of touchdown, respectively in the x and y directions, respectively. Similarly, x_2^* and y_2^* are the positions of the aircraft on the runway, after the instant of touchdown, in the moving load phase. x_2^* and y_2^* can be found as in (18), (19);

$$X_2^* = X_1^* + V_H \cdot t \qquad (18)$$

$$Y_2^* = Y_1^* \qquad (19)$$

where V_H is the horizontal landing velocity of the aircraft in x direction.

B. Numerical Solution

For the numerical (finite element method) solution of the given problem, ABAQUS/Standard is used. The problem is solved by using an implicit analysis. The tire used in numerical modeling includes a rubber part, a reinforcing ply, a steel bead and a rim as shown in Figs. 3 (a)-(d). The materials for the reinforcing ply, steel bead, and the rim are taken as steel, whereas a hyperelastic rubber material model is used for the rubber, which also has viscoelastic material properties. The material properties of the steel and rubber are given as in the Table II [13], where C_{10}, C_{01} and D_1 are temperature dependent material parameters of Mooney-Rivlin hyperelastic material model; and $\bar{g}_i^p$ is the shear relaxation modulus ratio, $\bar{k}_i^p$ is the bulk relaxation modulus ratio, and τ_i is the relaxation time properties of Prony parameters of the viscoelastic material model of the rubber.

The reinforcing ply of the aircraft tire is modeled as shell, while the rubber and the bead parts are modeled as solid parts. The runway is modeled as a composite plate composed of four layers, by using the materials given in Table I. The reinforcing ply and the bead parts are embedded within the tire by using the constraint manager in the ABAQUS.

The mass of the aircraft is defined as a point mass above the tire. To simulate the tire's response to a landing of aircraft realistically, the mass of aircraft, which is modeled by using a point mass, is connected to the tire via a spring and a dashpot as if landing gear (Fig. 5). Similarly, spring and dashpot connections are also used between the soil and the runway to model the soil as Pasternak type foundation (Fig. 6).
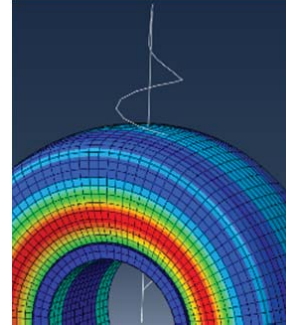

Fig. 5 The spring and the dashpot between the aircraft point mass and the tire

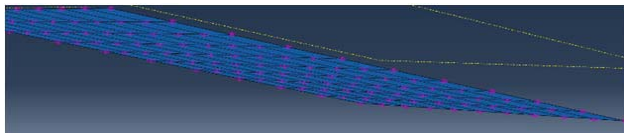| Material	Density (kg/m³)	Young's Modulus (GPa)	Poisson's Ratio	Hyperelastic	Viscoelastic
Steel	5900	172.2	0.3	-	-
Rubber	1100	87.52	0.22	$C_{10}=10^6$, $C_{01}=0$, $D_1=5\times10^{-8}$	$\bar{g}_i^p = 0.3$, $\bar{k}_i^p = 0$, $\tau_i=0.1$

Fig. 6 The spring and dashpot connections between the runway and the soil

The ABAQUS analysis consists of two parts. In the first part, a pressure of 1.3 MPa is applied to the tire and inflated in a Static step. Then in the second analysis, an implicit procedure is defined, in which the aircraft is given a horizontal and a vertical initial velocity and impacted to the runway. The boundary condition of the runway is taken as simply supported

along its four edges. 37,372 elements and 46,722 nodes are used to create the mesh structure of the tire with its all constituents, while 1800 elements and 1877 nodes are used for meshing the composite runway.

Numerical solutions for the maximum pressure and the maximum deformations those occur on the runway are obtained. The vertical (V_v) and horizontal (V_H) aircraft velocities, the volume fraction (VF) of the steel material in the reinforced concrete layer only, and the impact location of the tire (y^*) on the runway are taken as 0.3 m/s, 40 m/s, 0.2 and 2 m., respectively, for the base case. The parameters that are investigated in this study are given in Table III.

TABLE III
PARAMETERS INVESTIGATED IN THIS STUDY

Parameter	V_v (m/s)	V_H (m/s)	VF	y^* (m/s)
The vertical velocity (V_v) of the tire	0.3, 0.4, 0.5, 0.6, 0.7, 0.8, 0.9, 1	40	0.2	2
The horizontal velocity (V_H) of the tire	0.3	40, 42, 44, 46, 48, 50	0.2	2
VF of the Steel Material Inside the Reinforced Concrete Layer	0.3	40	0.1, 0.2, 0.3, 0.4, 0.5	2
The impact location (y^*) of the tire to the runway	0.3	40	0.2	0, 0.5, 1, 1.5, 2

V. RESULTS AND DISCUSSION

The maximum pressure and deformations responses of the runway under the impact and moving load are obtained for different; vertical and horizontal velocities of the tire, VFs of the steel material inside the reinforced concrete layer and impact locations of the tire to the runway.

The change of the maximum pressure on the runway with the vertical impact velocity of the tire, which is read from the ABAQUS analysis, is given in Fig. 7.
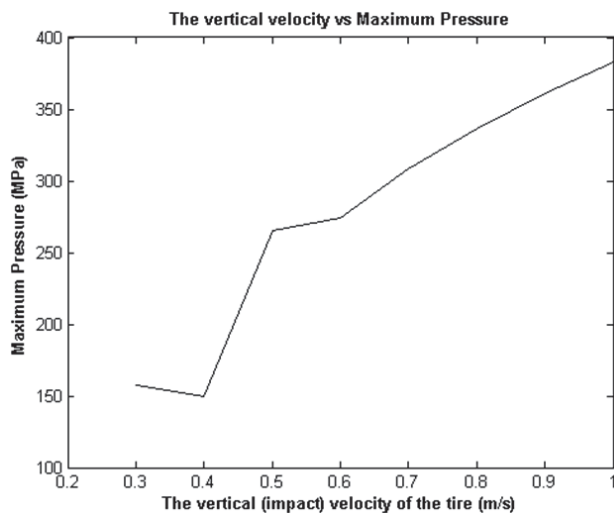

Fig. 7 The effect of the vertical impact velocity of the tire on the maximum pressure response on the runway

As it can be seen from Fig. 7, the maximum pressure on the runway increases as the vertical impact velocity of the tire increases.

The change of the maximum non-dimensional deflection of the runway with the changing vertical impact velocity of the tire, obtained from ABAQUS (finite element method, numeric solution) and MATLAB (analytic) analyses is given in Fig. 8.
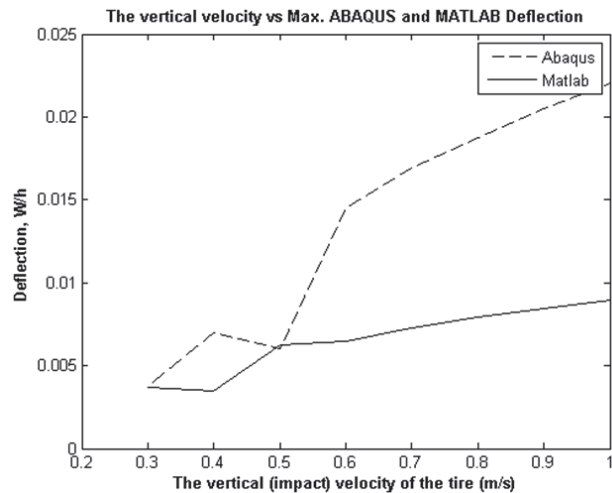

Fig. 8 The effect of the vertical impact velocity of the tire on the maximum deflection response of the runway

As it is seen in Fig. 8, the maximum deformation within the plate increases with the increasing vertical impact velocity of the tire. It can be seen that the maximum deformation within the runway is a thousandth of the runway thickness, in average, which is in the acceptable range. Also, ABAQUS and MATLAB solutions are in with great accordance with each other.
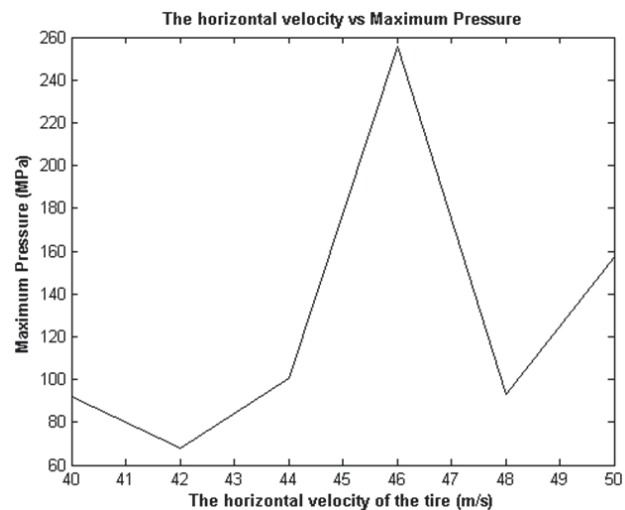

Fig. 9 The change of the maximum pressure with the horizontal aircraft velocity

The variation of the maximum pressure on the runway with the horizontal velocity of the aircraft, which is read from the ABAQUS post processing, is given in Fig. 9.

The maximum pressure, given in Fig. 9, occurs at the location, where the tire impacts the runway, for the tire horizontal velocity of 46 m/s. The reasons for the peak pressure at the horizontal velocity of 46 m/s may be the approximate nature of the implicit analysis which may not be proper for the present problem or the natural frequencies of the soil-runway assembly may be close to excitation frequency of the landing dynamic forces, which are the function of the landing speed. From 40 m/s to the 50 m/s of horizontal velocities, a slight increase in the maximum pressure value can be observed.
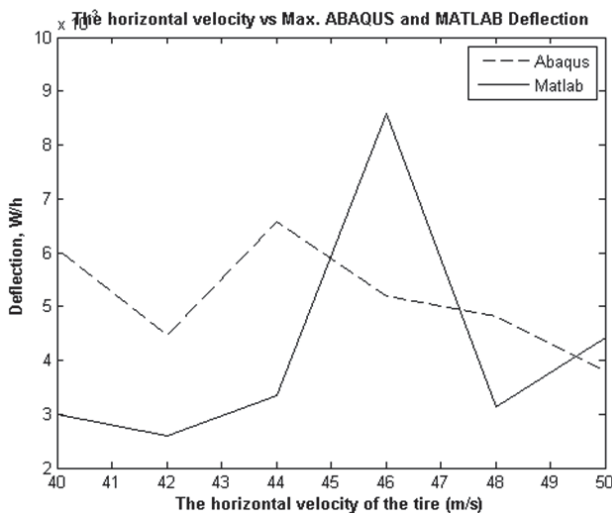

Fig. 10 The effect of the horizontal velocity of the tire on the maximum deflection response of the runway
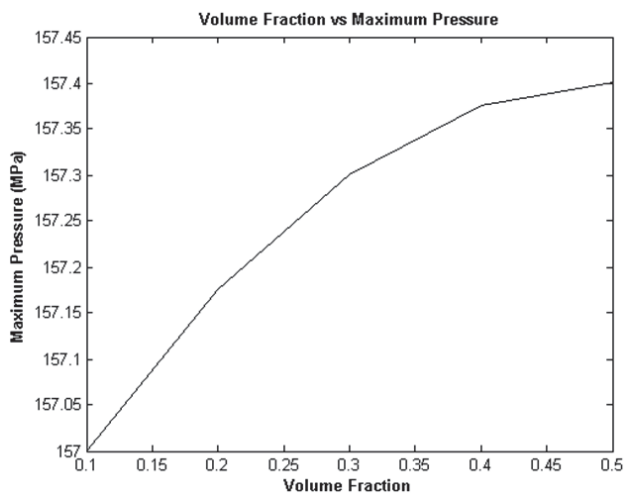

Fig. 11 The change of the maximum pressure on the runway with the VF of the steel material inside the reinforced concrete layer

The change of the maximum non-dimensional deflection of the runway with the changing horizontal velocity of aircraft,

obtained from ABAQUS and MATLAB analyses is given in Fig. 10.

As it can be seen from Fig. 10, the maximum non-dimensional deflections within the runway are similar to each other for the ABAQUS and the MATLAB solutions. The two results show similar behavior, with a slight time lag only. The time lag between the results is caused mainly by the nature of the implicit analysis in ABAQUS, and/or by the inaccuracy in precisely reading the ABAQUS results for any time.

The change of the maximum pressure on the runway with the VF of the steel material inside the reinforced concrete layer of the runway, which is read from the ABAQUS analysis, is given in Fig. 11.

It can be seen from Fig. 11 that the maximum pressure at the instant of touchdown increases with the increasing steel VF. As the second layer, and the runway in overall, is getting stiffer against bending with the increasing steel VF, the impact energy causes more stresses at the instant of touchdown. Although, the change in the peak pressure values is negligible.

The change of the maximum non-dimensional deflection of the runway with the changing steel VF in the reinforced concrete layer, obtained from ABAQUS and MATLAB analyses is given in Fig. 12.
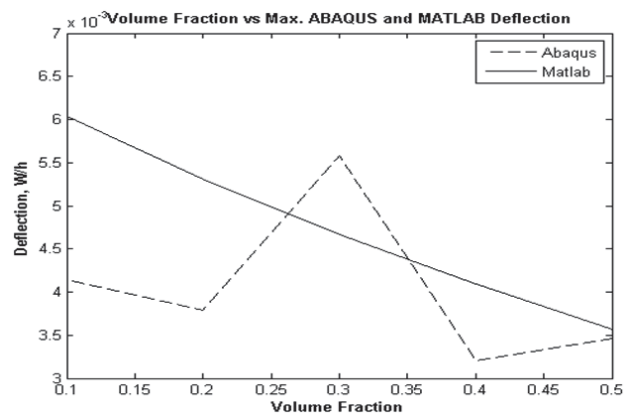

Fig. 12 The change of the maximum deflection on the runway with the VF of the steel material inside the reinforced concrete layer

As it can be seen from Fig. 12, the maximum non-dimensional deflection within the plate decreases with the increasing steel VF in the reinforced concrete layer of the runway. Since the strength and stiffness of the runway improves with the increased steel VF, it becomes more resistant to bending and the deflection response becomes lower, as expected.

The change of the maximum non-dimensional deflection of the runway with the impact distance from the side of the runway, obtained from ABAQUS and MATLAB analyses is given in Fig. 13. The impact distance of 0 m. means that the tire hits the runway on its side boundary, and the impact distance of 2 m. means that the tire hits the middle line of the runway between the two side boundaries.
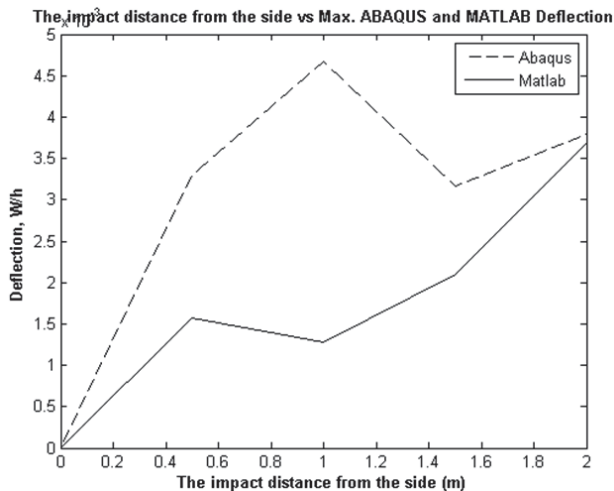
Fig. 13 The effect of the impact distance from the side on the deflection response of the runway

The deflection responses of the plate, given in Fig. 13, for both the ABAQUS and the MATLAB solutions, increases when the touchdown of the tire occurs nearer to the middle line of the runway. The trends for both the analytical and the numerical solutions are similar and the results are nearly the same. In both cases the non-dimensional responses are in the order of 10^{-3}.

VI. Conclusion

In the present study, the dynamics behavior of a moderately thick plate on Pasternak type foundation under impact and moving loads are investigated. A parametric study is conducted to examine the effects on the maximum pressures and deformations that occur within the runway by changing the vertical and the horizontal velocities of the tire, the VFs of the steel material inside the reinforced concrete, and the touchdown location of the tire.

Some important conclusions reached in this study are:
- The maximum pressure within the plate occurs at the instant of touchdown.
- The maximum pressure occurring within the plate increases as the horizontal and vertical velocities of the tire, and the VF of the steel inside the reinforced concrete layer increase.
- The deflection response of the runway becomes higher when the horizontal and vertical velocities of the tire is higher and the touchdown location of the tire is nearer to the mid-line of the runway.
- The deflection response becomes lower, as the steel VF in the reinforced concrete layer increases.

Some of the followings may be studied in the future:
- Running the FEM analysis by using the explicit method
- Creating a simpler model for the tire and its constituents
- Using multiple tires to model the landing aircraft more realistically
- Using different boundary conditions to examine its effects on the maximum pressure and deflection responses

- Investigating the effects of soil properties on the maximum pressure and deflection responses

References

[1] Bogacz, R., Czyczula, W., *Response of Beam on Visco-elastic Foundation to Moving Distributed Load.* Journal of Theoretical and Applied Mechanics, 2008. 46(4): p. 763-775.
[2] Özgan, K., Daloğlu, A., *Dynamic Response of Thick Plates on Two Parameter Elastic Foundation under Time Variable Loading.* International Journal of Engineering and Applied Sciences, 2014. 4: p. 40-51.
[3] Idowu, A.S., Are, E.B., Joseph, K.M., Daniel S.K, *Dynamic Effects of Viscous Damping on Isotropic Rectangular Plates Resting on Pasternak Foundation, Subjected to Moving Loads.* International Journals of Mathematics and Statistical Studies, 2013. 1(2): p. 12-19.
[4] Gibigaye, M., et al., *Dynamic Response of a Rigid Pavement Plate Based on an Inertial Soil.* International Scholarly Research Notices, 2016. 2016: p. 9.
[5] Maamar, D.B., Zenasni, R., Hebbar, A., Olay, J.V., *Finite Element Modeling of Composite Materials Subjected to the Low Velocity Impact Damage.* American Journal of Materials Science, 2013. 3(1): p. 1-7.
[6] Lee, J., Kong, C., Soutis, C., *Modelling of Low Velocity Impact Damage in Laminated Composites.* Journal of Mechanical Science and Technology, 2005. 19(4): p. 947-957.
[7] Abdesssemed, M., S. Kenai, and A. Bali, *Experimental and numerical analysis of the behavior of an airport pavement reinforced by geogrids.* Construction and Building Materials, 2015. 94: p. 547-554.
[8] Vosoughi, A.R., P. Malekzadeh, and H. Razi, *Response of moderately thick laminated composite plates on elastic foundation subjected to moving load.* Composite Structures, 2013. 97: p. 286-295.
[9] BOEING, *Airport Reference Code and Approach Speeds for Boeing Airplanes.* 2011.
[10] Jingzhe, J., *A Mixed Mode Function - Boundary Element Method for Very Large Floating Structure - Water Interaction Systems Excited by Airplane Landing Impacts*, in *School of Engineering Sciences, Ship Science.* 2007, University of Southampton.
[11] BOEING, *747-400 Airplane Characteristics for Airport Planning.* 2002. p. 157.
[12] Reddy, J.N., *Mechanics of Laminated Composite Plates and Shells: Theory and Analysis.* 2004, Boca Raton, Florida: CRC Press.
[13] Dassault Systemes, *Abaqus 6.11 Documentation, Abaqus Example Problems Manual, Tire and Vehicle Analyses.* 2011.